

Solidification study of Cu-based alloys obtained by continuous casting

M. T. CLAVAGUERA-MORA*, C. COMAS, J. L. TOURON

Grup de Física de Materials I, Dept. de Física, Universitat Autònoma de Barcelona, 08193-Bellaterra, Spain

M. GARCÍA, O. GUIXÀ

La Farga Lacambra, 08519-Les Masies de Voltregà, Spain

N. CLAVAGUERA

Grup de Física de l'Estat Sòlid, Dept. d'ECM, Facultat de Física, Universitat de Barcelona, Diagonal 647, 08028-Barcelona, Spain

E-mail: narcis@ecm.ub.es

Commercial production of copper by continuous casting in a wheel-and-band machine, with suitable modifications to induce high undercooling, is considered. Impurities control to a large extent the microstructure and mechanical properties of the ingot. Suitable solute additives in the molten alloy to achieve constitutional supercooling during solidification have been analyzed, with particular emphasis on the presence of lead. Experimental information on the Cu-O-Pb phase diagram has been revised and modeling of the microstructure evolution as a function of several casting parameters is being presented.

© 1999 Kluwer Academic Publishers

1. Introduction

Solidification in the casting process is largely determined by thermodynamic and kinetic factors. From the kinetic point of view, solidification results in an abrupt decrease of atomic mobility. Since the raw material is initially in the molten state, the heat release is large, which means that large amounts of heat have to be extracted quickly. The microstructure of the cast product (i.e. second-phase particle distribution parameters such as secondary dendrite arm spacing, particle and/or eutectic colony size, and matrix composition, etc.) is mostly determined by both phase diagram equilibrium and kinetic considerations, in particular the liquid composition and casting procedure. In the commercial production of Cu by the Properzi process, a copper bar is continuously cast on a wheel-and-band machine [1]. Copper solidifies in the gap as the wheel and band rotate through a portion of circular path. Casting rates are typically of 30 tons/h for a 53×39 mm copper billet. Phase diagram and thermodynamic data are of considerable fundamental and practical interest to check the influence of the liquid composition. In particular, the role of Pb impurities in the solidification process is important because this element is immiscible in solid Cu [2].

In this paper a series of rich Cu alloys obtained by the Properzi process are analyzed. Their solidification behaviour as a function of composition is described in terms of microscopic observations. The phase equilibrium in the pseudo ternary system Cu-Cu₂O-

PbO-Pb is revised and the role of liquid composition in the resulting microstructure after continuous casting of Cu is established.

2. Microstructural analysis

Typically, casting of Cu with impurity contents ranging between 100–300 ppm O and 200–600 ppm Pb produces the predominant nucleation at, or close to, the wheel-and-band wall, resulting in a columnar-grown zone because the crystals advance rapidly when the growth direction is parallel and opposite to the heat flow direction. Beyond a certain stage in the solidification development, a transition from columnar to equiaxed region occurs which is highly dependent on the casting conditions. Fig. 1 shows a typical optical microscope view of the longitudinal and transverse bar sections. Scanning electronic microscopic observations (see Figs 2 and 3) indicate that equiaxed Cu grains have diameters varying from 5 to 100 μm whereas eutectic Cu + Cu₂O colonies are located at grain boundaries and in interdendritic pockets, their size being of 0.1 to 1 μm . PbO grains appear mostly in the central region of the bar.

The microstructural analysis indicates that two ranges of composition domains may be distinguished according to the value of the Pb/O ratio content.

a) Samples with a low Pb/O ratio content exhibit eutectic colonies with irregular grain sizes of the Cu₂O

* Author to whom all correspondence should be addressed: M. T. Clavaguera-Mora, Grup de Física de Materials I, Dept. de Física, Universitat Autònoma de Barcelona, 08193-Bellaterra, Spain.

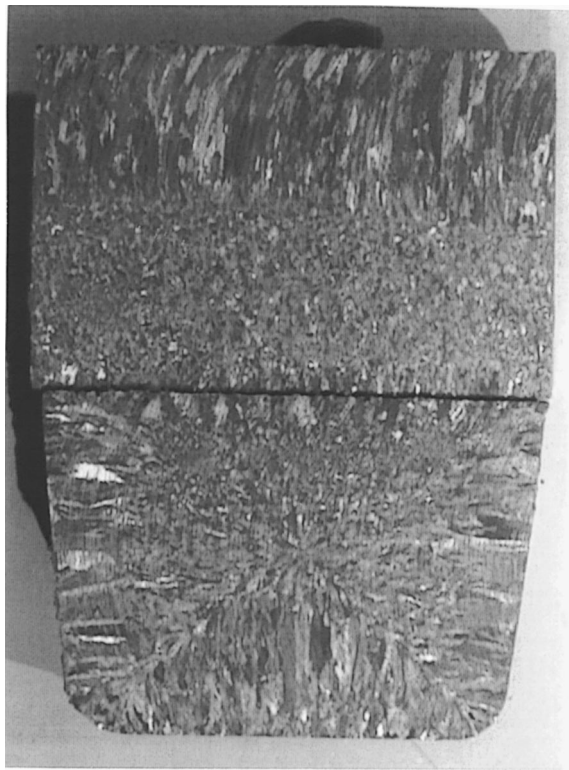


Figure 1 General view of the vertical and horizontal sections of the bar produced after casting by the Properzi process.

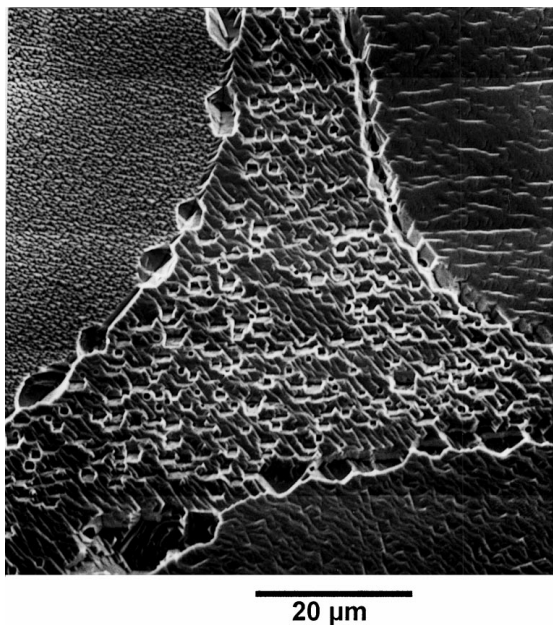


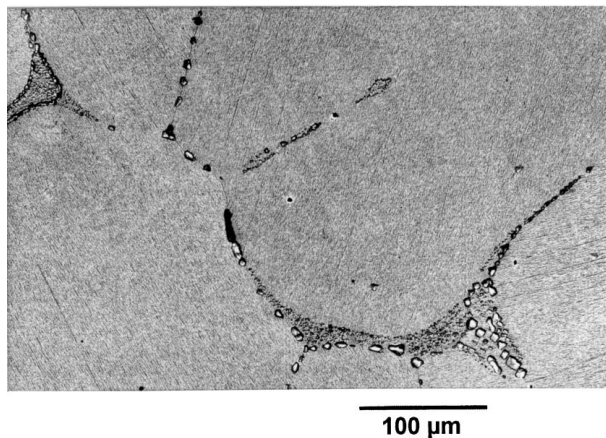
Figure 2 Micrograph of a sample with 80 ppm Pb and 240 ppm O. Eutectic phase in between adjacent Cu grains.

precipitates and no trace of coexistence of two immiscible liquids in the solidification process (Figs 2 and 3).

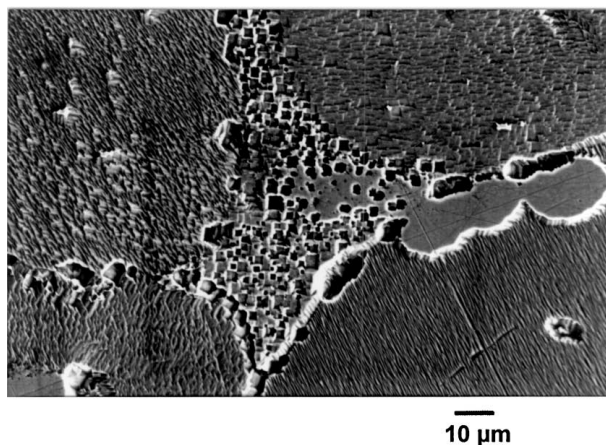
b) Samples with a high Pb/O ratio content exhibit in some of the equiaxed or columnar Cu grains a fine dispersion and coalescence of droplets which may be the signature of a liquid-liquid immiscibility in the solidification path (Fig. 4).

2.1. The Cu-Cu₂O-PbO-Pb pseudo ternary system

According to the microstructural analysis, the location of some invariant points in the phase diagram is



(a)



(b)

Figure 3 Micrograph of a sample with 160 ppm Pb and 140 ppm O: (a) eutectic at the grain boundary results in Cu₂O particles; (b) irregular eutectic with some large Cu₂O grains.

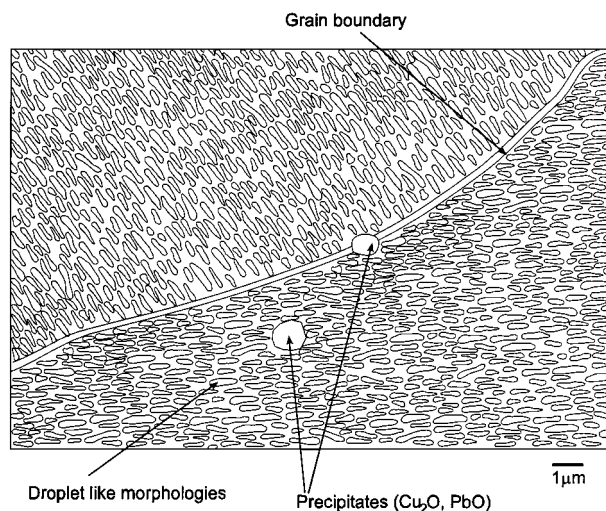


Figure 4 Sketch showing the final microstructure generated by the L1 + L3 immiscibility.

proposed. The general phase equilibrium follows the lines given by Chang and Hsieh [3]. Experimental information comes from the bibliography [2, 4–8] and the results obtained in the present work. The representation of the equilibrium in condensed phases in the Cu-O-Pb system bounded by Cu-Cu₂O-PbO-Pb is presented in Fig. 5 as the projection of the monovariant reactions in the orthogonal composition plane. In this

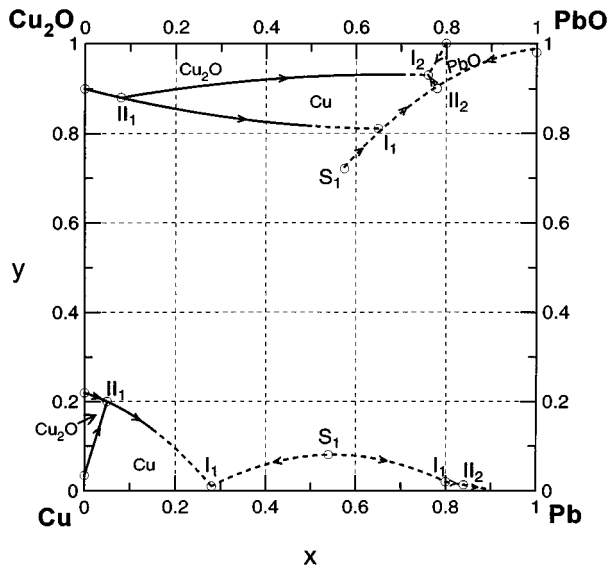


Figure 5 Projection of the invariant equilibrium of the pseudo ternary system Cu-Cu₂O-PbO-Pb. The primary crystallization fields of each crystalline phase are also indicated.

representation the co-ordinates (x , y) of a point correspond to the global fraction of cations and anions defined by the following equations:

$$\begin{aligned} x &= n_{\text{Pb}} / (n_{\text{Pb}} + 1/2n_{\text{Cu}}) \\ y &= n_{\text{O}} / (n_{\text{Pb}} + 1/2n_{\text{Cu}}) \end{aligned} \quad (1)$$

where n_{O} , n_{Pb} and n_{Cu} are the number of moles of anions and cations of the different elements present in each ternary composition.

3. Discussion

According to the phase reaction scheme shown in Table I, solidification under equilibrium in Cu-rich alloys is mainly determined by the invariant reaction II₁ (see also Fig. 5), namely: $L1_{\text{II}_1} + \text{Cu}_2\text{O} \rightleftharpoons (\text{Cu})_{\text{II}_1} + L3_{\text{II}_1}$, since alloys with a Pb/O weight ratio content either higher or lower than ≈ 1.1 will have an excess of $L1_{\text{II}_1}$ or Cu_2O at the end of that reaction, respectively. We will comment successively on the consequences of the value of the Pb/O weight ratio in the molten alloys on the microstructure of the resulting cast material.

Molten alloys with a Pb/O weight ratio content lower than about 1.1 will form primary Cu crystals followed by eutectic $\text{Cu} + \text{Cu}_2\text{O}$ formation from a Cu rich liquid, $L1$, down to 1040°C . At this temperature reaction II₁ takes place and $L1$ is consumed, with some Cu_2O , to increase solid Cu and form $L3$. Subsequent solidification of the $L3$ liquid follows the eutectic monotectic line $\text{II}_1 \rightarrow \text{II}_2$ where the eutectic mixture $\text{Cu} + \text{Cu}_2\text{O}$ forms from an O enriched liquid, $L3$, until this liquid transforms to the solid phases at 677°C . Non-equilibrium solidification results in partial transformation at 1040°C and, consequently, irregular eutectic mixture distribution over the casting product. Fig. 6 shows the sequence of phases appearing during the solidification of two selected alloy compositions. Such figure has been constructed by application of the lever rule to the solidification path, depicted in Fig. 5. Below 1040°C there is an increase in the amount of Cu_2O formed by the eutectic reaction from the O rich liquid $L3$. As a consequence, the cast product has Cu_2O particles, irregular in shape and size, surrounding the Cu grains, as depicted in Figs 2 and 3.

On considering the solidification path in molten alloys with a Pb/O weight ratio content higher than about

TABLE I Invariant phase equilibrium scheme

Cu-O	Cu-Pb	Cu-O-Pb	Pb-O	Cu ₂ O-PbO
$m_1: 1223^\circ\text{C}$ $L3_{m_1} \rightleftharpoons L1_{m_1} + \text{Cu}_2\text{O}$ $e_1: 1066^\circ\text{C}$ $L1_{e_1} \rightleftharpoons (\text{Cu})_{e_1} + \text{Cu}_2\text{O}$	$m_2: 955^\circ\text{C}$ $L1_{m_2} \rightleftharpoons L2_{m_2} + (\text{Cu})_{m_2}$	$\text{II}_1: 1040^\circ\text{C}$ $L1_{\text{II}_1} + \text{Cu}_2\text{O} \rightleftharpoons (\text{Cu})_{\text{II}_1} + L3_{\text{II}_1}$ $\text{I}_1: 954^\circ\text{C}$ $L1_{\text{I}_1} \rightleftharpoons L2_{\text{I}_1} + L3_{\text{I}_1} + (\text{Cu})_{\text{I}_1}$ $\text{II}_2: 847^\circ\text{C}$ $L2_{\text{II}_2} + L3_{\text{II}_2} \rightleftharpoons (\text{Cu})_{\text{II}_2} + \text{PbO}$ $\text{I}_2: 677^\circ\text{C}$ $L3_{\text{I}_2} \rightleftharpoons (\text{Cu})_{\text{I}_2} + \text{Cu}_2\text{O} + \text{PbO}$ $\text{I}_4: 325^\circ\text{C}$ $L2_{\text{I}_4} \rightleftharpoons (\text{Cu})_{\text{I}_4} + (\text{Pb})_{\text{I}_4} + \text{PbO}$	$m_3: 870^\circ\text{C}$ $L3_{m_3} \rightleftharpoons L2_{m_3} + \text{PbO}$	$e_4: 680^\circ\text{C}$ $L3_{e_4} \rightleftharpoons \text{Cu}_2\text{O} + \text{PbO}$
	$e_2: 326^\circ\text{C}$ $L2_{e_2} \rightleftharpoons (\text{Cu})_{e_2} + (\text{Pb})_{e_2}$		$e_3: 327^\circ\text{C}$ $L2_{e_3} \rightleftharpoons (\text{Pb})_{e_3} + \text{PbO}$	

$L1_{\text{II}_1}$ and $L3_{\text{II}_1}$ have, respectively, 2.4 wt % O and 8 wt % Pb, and 9 wt % O and 10 wt % Pb.

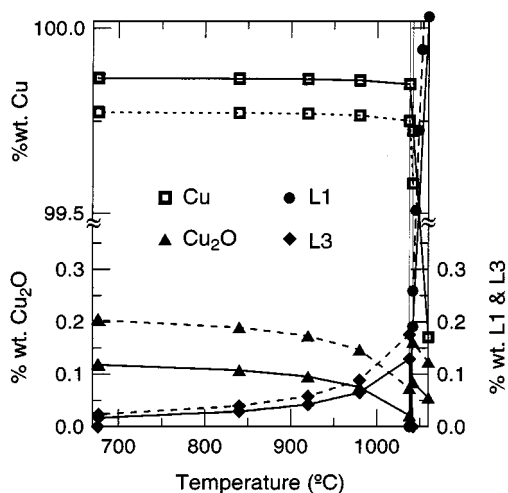


Figure 6 Phases appearing during the solidification of alloys with 150 ppm Pb and 200 ppm O (solid lines) and with 200 ppm Pb and 300 ppm O (dashed lines).

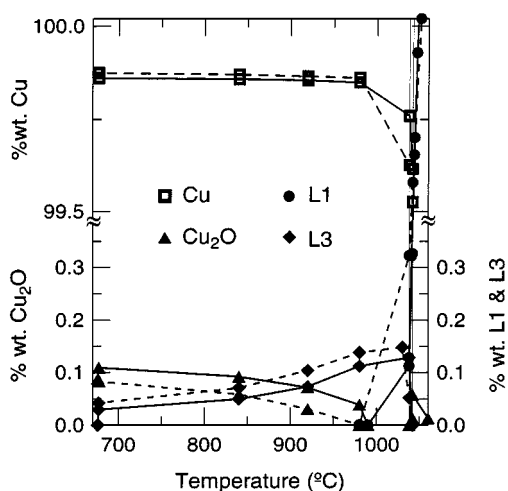


Figure 7 Phases appearing during the solidification of alloys with 250 ppm Pb and 200 ppm O (solid lines) and with 350 ppm Pb and 100 ppm O (dashed lines).

1.1 the first steps, namely primary crystallization of Cu followed by eutectic Cu + Cu₂O formation, are identical to those already described. However, at 1040 °C, reaction II₁ under equilibrium conditions leaves some amount of L1 unreacted which coexists with L3 and is further consumed to the expense of Pb enrichment of L3 and Cu precipitation until line II₁ → I₂ is reached. Fig. 7 depicts the situation for two selected alloy compositions. Under casting production, again some unreacted Cu + Cu₂O eutectic mixture formed above 1040 °C re-

mains below that temperature, but, more significantly for practical purposes, the eutectic reaction continues at a temperature much below 1040 °C, that is, at increasing undercooling, and consequently the remaining liquid has a negligible probability to be distributed over large pockets. Therefore, large Cu₂O particles are avoided at the Cu grain boundaries. Further, the coalescence of the immiscible droplets produces a fine dispersion as well as Cu₂O precipitates inside the grains, as shown in Fig. 4.

4. Conclusions

Commercial production of copper by continuous casting in a wheel-and-band machine, with suitable modifications to induce high undercooling, has been considered. The Pb impurities control to a large extent the microstructure of the casting product and affect the mechanical properties of the ingot.

Experimental information on the Cu-O-Pb phase diagram has been revised and modeling of the microstructure evolution as a function of several casting parameters has been presented. Suitable Pb/O weight ratio amounts in the molten alloy to achieve specific microstructures after solidification have been analyzed.

Acknowledgements

Support of La Farga Lacambra through an OTRI/UAB project and from CICYT projects MAT96-0769 and MAT96-0692 is acknowledged. Author JLT wants to acknowledge support from Commissionat per a Universitats i Recerca (CIRIT—Generalitat de Catalunya).

References

1. M. S. STANFORD, *Copper* **1** (1967) 11.
2. J. NIEMELA, *Calphad* **10** (1986) 77.
3. Y. A. CHANG and K.-C. HSIEH, "Phase Diagrams of Ternary Copper-Oxygen-Metals Systems" (ASM, Metals Park, Ohio, 1989) pp. 95–106.
4. *Metals Handbook*, Vol. 8, Metallography, Structures and Phase Diagrams, 8th ed. (ASM, Metals Park, Ohio, 1973).
5. M. F. ABADIR, A. M. GADALLA and Y. M. EL-AGAWI, *Trans. Br. Ceram. Soc.* **75** (1976) 68.
6. E. GEBHARDT and W. OBROWSKI, *Z. Metallk.* **45** (1954) 332.
7. A. M. GADALLA, *Sci. Ceram.* **3** (1967) 179.
8. J. GERLACH, H. J. KLEIBELER and F. PAWLEK, *Metall.* **21** (1967) 1115.

Received 3 March 1997

and accepted 27 October 1998